

The electronic structure of β -HgS via *GW* calculations

Bradford A. Barker^{1,2,3} and Steven G. Louie^{2,3}

¹*Department of Physics, University of California, Merced, CA 95343, USA*

²*Department of Physics, University of California, Berkeley, CA 94720, USA*

³*Materials Sciences Division, Lawrence Berkeley
National Laboratory, Berkeley, CA 94720, USA*

(Dated: March 31, 2022)

Abstract

The electronic structure of the zincblende β -HgS is not well understood. Previous first-principles calculations using fully-relativistic density functional theory and many-body perturbation theory in the fully-relativistic GW approach have predicted an inverted, topologically non-trivial ordering of these states, with the s -like Γ_6 state occupied. However, other calculations using the GW approach in which spin-orbit coupling is added perturbatively (“ $GW+SOC$ ”) predict the p - d hybridized Γ_7 and Γ_8 states to be occupied and the Γ_6 state to be unoccupied, suggesting that β -HgS is a topologically trivial small band gap semiconductor. In the present work, a plane-wave pseudopotential fully-relativistic GW calculation finds a band ordering in agreement with the previous $GW+SOC$ calculations. The calculated band gap is 0.10 eV and the electron effective mass is $0.07 m_e$, in good agreement with experiment.

I. INTRODUCTION

Metacinnabar, or β -HgS, has a zincblende structure and large spin-orbit coupling. The related mercury chalcogenide zincblende solids HgSe and HgTe have a semimetallic, α -Sn-like bandstructure, with parabolic valence and conduction bands degenerate at the Γ -point. For α -Sn, HgSe, and HgTe, the bands near the Fermi level at the Γ -point have an inverted bandstructure: The order of states, in increasing energy, for a conventional zincblende system is the $p_{1/2}$ -like Γ_7 , $p_{3/2}$ -like Γ_8 , and s -like Γ_6 , while HgSe and HgTe place Γ_6 lowest in energy, then Γ_7 , then Γ_8 . Furthermore, the four-fold degenerate Γ_8 splits into a pair of parabolic valence and conduction bands, degenerate at the Γ -point. This behavior in the bandstructure for these materials is in agreement in the literature, regardless of the details by which spin-orbit coupling is incorporated.[1–3]

The bandstructure for β -HgS, however, has seen considerable disagreement between different theoretical calculations and experiment. The α -Sn-like inverted bandstructure was proposed to be consistent with experimental measurements [4]. Reflectivity data indicates a plasma edge at 0.10 eV[4], suggesting a metallic or semimetallic nature. Absorption data indicated an onset of interband transitions at 0.25 eV, interpreted as the onset of transitions to a partially occupied, zero-gap parabolic conduction band[4]. In the absence of ARPES spectra, however, there is not a definitive experimental description of the quasiparticle bandstructure.

Density functional theory calculations[5, 6], however, indicate a small indirect band gap and states ordered $\Gamma_6, \Gamma_8, \Gamma_7$ [7]. Compared to HgSe and HgTe, there is a further inversion between Γ_8 and Γ_7 , with Γ_8 now being fully occupied even away from the Γ -point. Based on the fully-relativistic DFT bandstructure, β -HgS has been predicted to be a nontrivial Z_2 insulator much like strained HgTe, with highly anisotropic topologically protected Dirac surface states along the [001] direction[8, 9]. Topological properties based on the ordering of bands near the Fermi energy need to be confirmed from calculations that are more accurate than DFT[10], which is well-known to underestimate band gaps. Many-body perturbation theory in the GW approximation provides physically accurate excited-state properties such as the electronic bandstructure. GW calculations in which the spin-orbit coupling Hamiltonian is applied as a perturbation to the quasiparticle energies (“ GW +SOC”) predict a band ordering of $\Gamma_8, \Gamma_7, \Gamma_6$ [2, 11], which is similar to that of CdTe, but with the p - d hybridized orbitals Γ_8 and Γ_7 inverted, due to the strength of SOC in the Hg $5d$ states. This ordering of states yields a topologically trivial band gap, as the bandstructure can be adiabatically deformed to that of the topologically trivial CdTe[12] without closing the bulk band gap by, e.g., tuning the atomic spin-orbit parameters of Hg and S.

Previous GW calculations in which spin-orbit coupling is incorporated non-perturbatively through the use of fully-relativistic pseudopotentials for the Kohn-Sham equations and spinor wavefunctions in the construction of the self-energy (“FR- GW ”) yield the same band ordering as in DFT[3, 13].

The disagreement in the various computed quasiparticle bandstructure topologies is curious, since the fully-relativistic DFT (“FR-DFT”) bandstructures are all in agreement despite the different choices of basis sets. In this work, the FR- GW quasiparticle bandstructure is calculated using a plane-wave basis and approximating the electron-ion interaction within the Local Density Approximation (LDA)[14] when constructing fully-relativistic pseudopotentials for the Kohn-Sham wavefunction calculations. These wavefunctions are used as the basis for the quasiparticle bandstructure calculations. In Section II the method of “one-shot” FR- GW in a plane-wave basis is reviewed, and in Section III the electronic structure is discussed.

II. METHODS

The Hedin equations with the inclusion of spin-orbit coupling, within the GW approximation, are[15]

$$\begin{aligned}
W(\mathbf{r}_1, \mathbf{r}_2; \omega) &= v(\mathbf{r}_1, \mathbf{r}_2) + \int d\mathbf{r}_3 d\mathbf{r}_4 d\omega' v(\mathbf{r}_1, \mathbf{r}_3) P(\mathbf{r}_3, \mathbf{r}_4; \omega') W(\mathbf{r}_4, \mathbf{r}_2; \omega - \omega'), \\
P(\mathbf{r}_1, \mathbf{r}_2) &= -\frac{i}{2\pi} \sum_{s_1, s_2} \int d\omega' G(\mathbf{r}_1, s_1, \mathbf{r}_2, s_2; \omega + \omega') G(\mathbf{r}_2, s_2, \mathbf{r}_1, s_1; \omega'), \\
\Sigma(\mathbf{r}_1, s_1, \mathbf{r}_2, s_2; \omega) &= \frac{i}{2\pi} \int d\omega' e^{-i0^+\omega'} G(\mathbf{r}_1, s_1, \mathbf{r}_2, s_2; \omega - \omega') W(\mathbf{r}_1, \mathbf{r}_2; \omega'), \\
\Gamma(\mathbf{r}_1, s_1, \mathbf{r}_2, s_2, \mathbf{r}_3) &= \delta(\mathbf{r}_1 - \mathbf{r}_2)\delta(\mathbf{r}_2 - \mathbf{r}_3)\delta_{s_1, s_2}
\end{aligned} \tag{1}$$

with the one-particle Green's function constructed using Kohn-Sham energies, $\epsilon_{n\mathbf{k}}$, and orbitals[3, 16], $\phi_{n\mathbf{k}\alpha}(\mathbf{r})$,

$$G(\mathbf{r}_1, s_1, \mathbf{r}_2, s_2; \omega) \approx \sum_{n\mathbf{k}} \frac{\phi_{n\mathbf{k}}(\mathbf{r}_1, s_1)\phi_{n\mathbf{k}}^*(\mathbf{r}_2, s_2)}{\omega - \epsilon_{n\mathbf{k}} - i\delta_{n\mathbf{k}}}, \tag{2}$$

where $\delta_{n\mathbf{k}} = 0^+$ for $\epsilon_{n\mathbf{k}} < \mu$ and $\delta_{n\mathbf{k}} = 0^-$ for $\epsilon_{n\mathbf{k}} > \mu$.

The Kohn-Sham energies and orbitals are calculated using Quantum ESPRESSO[17], with fully-relativistic pseudopotentials for Hg and S generated from the Optimized Norm-Conserving Vanderbilt Pseudopotential method[18] with parameters adapted from the Pseudo-Dojo pseudopotential database[19, 20]. The Hg pseudopotential includes the $5s^25p^65d^{10}$ semicore states as valence for accurate calculation of the bare exchange matrix elements [21]. A kinetic energy cutoff of 200 Ry and an $8 \times 8 \times 8$ Monkhorst-Pack grid are used for calculating the charge density and the relaxed structural geometry. The relaxed lattice parameter is calculated to be identical to the experimental value of 5.85 Å [22].

The calculation for the polarizability is identical to the case in which spin-orbit coupling is neglected apart from the calculation of the plane-wave matrix elements (and any differences in the Kohn-Sham eigenvalues), where the spin degree of freedom appears as a trace:

$$M_{nn'}(\mathbf{k}, \mathbf{q}, \mathbf{G}) = \sum_s \langle n, \mathbf{k} + \mathbf{q}, s | e^{i(\mathbf{q} + \mathbf{G}) \cdot \mathbf{r}} | n', \mathbf{k}, s \rangle, \tag{3}$$

$$P_{\mathbf{G}\mathbf{G}'}(\mathbf{q}, \omega) = \sum_n^{\text{occ}} \sum_{n'}^{\text{unocc}} \sum_{\mathbf{k}} M_{nn'}^*(\mathbf{k}, \mathbf{q}, \mathbf{G}) M_{nn'}(\mathbf{k}, \mathbf{q}, \mathbf{G}') \frac{1}{2} \left[\frac{1}{\epsilon_{n\mathbf{k}+\mathbf{q}} - \epsilon_{n'\mathbf{k}} - \omega + i\delta} + \frac{1}{\epsilon_{n\mathbf{k}+\mathbf{q}} - \epsilon_{n'\mathbf{k}} + \omega + i\delta} \right].$$

The quasiparticle eigenvalues are the poles of Dyson's equation, which in the usual approximation where the Kohn-Sham orbitals are taken to be the quasiparticle orbitals gives

$$E_{n\mathbf{k}} = \epsilon_{n\mathbf{k}} + \sum_{s_1, s_2} \langle n, \mathbf{k}, s_1 | (\Sigma(s_1, s_2, E_{n\mathbf{k}}) - V^{\text{xc}} \delta_{s_1, s_2}) | n, \mathbf{k}, s_2 \rangle. \quad (4)$$

(The spatial dependence of Σ has been suppressed for brevity.) The calculation of the matrix elements of the self-energy is identical to that of the spinless case[23] apart from the trace over spin in the calculation of the plane-wave matrix elements $M_{nn'}$. In the usual screened-exchange/Coulomb-hole partitioning of the self-energy[16], the self-energy matrix elements[23, 24] to evaluate are

$$\begin{aligned} \sum_{s_1, s_2} \langle n, \mathbf{k}, s_1 | \Sigma^{\text{COH}}(s_1, s_2; \omega) | m, \mathbf{k}, s_2 \rangle &= \frac{i}{2\pi} \sum_{n'} \sum_{\mathbf{q}, \mathbf{G}, \mathbf{G}'} M_{n'n}^*(\mathbf{k}, -\mathbf{q}, -\mathbf{G}) M_{n'm}(\mathbf{k}, -\mathbf{q}, -\mathbf{G}') \\ &\times \int d\omega' \frac{\Im \epsilon_{\mathbf{G}\mathbf{G}'}^{-1}(\mathbf{q}; \omega')}{\omega - E_{n'\mathbf{k}-\mathbf{q}} - \omega' + i\delta} v(\mathbf{q} + \mathbf{G}'), \end{aligned} \quad (5)$$

$$\begin{aligned} \sum_{s_1, s_2} \langle n, \mathbf{k}, s_1 | \Sigma^{\text{SEX}}(s_1, s_2; \omega) | m, \mathbf{k}, s_2 \rangle &= \\ - \sum_{n'} \sum_{\mathbf{q}, \mathbf{G}, \mathbf{G}'}^{\text{occ}} M_{n'n}^*(\mathbf{k}, -\mathbf{q}, -\mathbf{G}) M_{n'm}(\mathbf{k}, -\mathbf{q}, -\mathbf{G}') \epsilon_{\mathbf{G}\mathbf{G}'}^{-1}(\mathbf{q}; \omega) v(\mathbf{q} + \mathbf{G}'). \end{aligned} \quad (6)$$

In this work, the polarizability is evaluated by explicitly calculating using the contour deformation method[25] with the static subspace approximation[26–28] with the BerkeleyGW[23] excited-state code modified for use with spinor wavefunctions. The dielectric matrix cutoff is 35 Ry, and 2000 unoccupied states are used for both the polarizability and Coulomb-hole sums. The error in the band gap due to the use of 2000 empty states in the Coulomb-hole sum is estimated to be 7 meV. An $8 \times 8 \times 8$ q-point grid for the dielectric function is used, as this grid has been shown to be sufficient for accurate calculations of the band gap for the similarly sized diamond-structure material, Ge[29]. For the static subspace approximation, the lowest 10 percent of the static dielectric matrix eigenvectors ($N_{\text{basis}} = 117$) gives a converged fundamental band gap within 6 meV. 15 imaginary frequencies for the contour deformation method give a band gap converged within 3 meV, compared to the use of 25 frequencies. The $\mathbf{q} \rightarrow 0$ limit is treated by the dual grid technique, appropriate for a semiconductor even with a small gap[23]. The quasiparticle energies calculated by the Hybertsen-Louie

Generalized Plasmon Pole model[16] (“GPP”) and the contour deformation method include the contributions from the static-remainder method[30] to estimate the correction from the missing bands from the finite Coulomb-hole sum.

III. ELECTRONIC STRUCTURE

The conventional band gap for a zincblende semiconductor is defined to be $E_0 = E(\Gamma_6) - E(\Gamma_8)$, which is positive for usual zincblende materials but negative for systems with band inversion. Likewise, the spin-orbit splitting $\Delta^{\text{SOC}} = E(\Gamma_8) - E(\Gamma_7)$ is also defined to be positive for the usual zincblende materials. However, the Hg $5d$ orbitals contribute to these states significantly, as p - d orbital hybridization is allowed for tetrahedral symmetries[31]. Since the Hg $5d_{5/2}$ state contributes to the Γ_7 and the Hg $5d_{3/2}$ to Γ_8 , Δ^{SOC} will be negative, as the spin-orbit splitting in these states (1.86 eV[32]) is much larger than that of the S $3p_{3/2}$ and $3p_{1/2}$ states (< 0.10 eV[33]).

The fully-relativistic DFT bandstructure is shown in Fig. 1. At Γ , spin-orbit coupling breaks the degeneracy at the Fermi level and opens a small spin-orbit gap, with the Γ_7 states unoccupied and the four-fold Γ_8 states occupied. The small indirect gap is 0.10 eV.

The quasiparticle energies within FR- GW approach are calculated for the Γ , $1/8 L$, $1/4 L$, $1/2 L$, $3/4 L$, L , $1/8 X$, $1/4 X$, $1/2 X$, $3/4 X$, and X -points. The bandstructure is then plotted with cubic splines, as the usual approach in which the quasiparticle bandstructure is linearly interpolated from the DFT bandstructure[23] requires the DFT bandstructure to be qualitatively similar to the quasiparticle bandstructure[23].

The states near the Fermi energy are ordered Γ_8 , Γ_7 , then Γ_6 , in agreement with other GW calculations in which spin-orbit coupling is added perturbatively[2, 11]. This is in contrast to the other reported FR- GW calculations in the literature[3, 13], where the states are ordered, as in DFT, Γ_6 , Γ_8 , then Γ_7 . The experimental band gap was estimated to be -0.11 eV from a Shubnikov-de Haas measurement of transition metal-doped samples of β -HgS, with the carrier concentration extrapolated to zero[34]. The model used to interpret the experiment, however, depends only on the absolute value of the band gap[35]. With the view that the experimental band gap may be positive, the calculated value of 0.10 eV is in good agreement. Similarly, the calculated electron effective mass to be $0.07 m_e$. This is in the range of values cited for the transition metal-doped β -HgS samples, $0.04 m_e$ to

0.07 m_e [34]. The electron effective mass estimated from reflectivity measurements also gives the value 0.07 m_e [4]. The gap at Γ has also been calculated with the frequency dependence of the self-energy treated by the COHSEX and Hybertsen-Louie Generalized Plasmon Pole model[16, 36] approximations, which give different values for the band gap but give the same order of the states. The band gaps are summarized in Table II.

To confirm the ordering of the states, off-diagonal COHSEX calculation was performed to estimate the degree by which the quasiparticle wavefunctions differ from the Kohn-Sham orbitals. The COHSEX approximation is a static approximation to the self-energy operator, and its frequency-independence allows for a completion relation to remove the sum over empty states in the Coulom-hole term in the self-energy:

$$\begin{aligned} \langle n, \mathbf{k}, s_1 | \Sigma^{\text{COH}}(s_1, s_2; \omega = 0) | m \mathbf{k} \beta \rangle = \\ \frac{1}{2} \sum_{\mathbf{q} \mathbf{G} \mathbf{G}'} \langle n, \mathbf{k}, s_1 | e^{i(\mathbf{G}' - \mathbf{G}) \cdot \mathbf{r}} \delta_{s_1, s_2} | m, \mathbf{k}, s_2 \rangle [\epsilon_{\mathbf{G} \mathbf{G}'}^{-1}(\mathbf{q}; \omega = 0) - \delta_{\mathbf{G} \mathbf{G}'}] v(\mathbf{q} + \mathbf{G}'). \end{aligned} \quad (7)$$

Thus COHSEX allows for rapid calculation of matrix elements of an approximate form of the self-energy operator.

The contribution of an Kohn-Sham orbital $\phi_{n\mathbf{k}}^{\text{KS}}(\mathbf{r})$ to the first-order correction to the COHSEX wavefunction $\psi_{n\mathbf{k}}^{(1)}(\mathbf{r})$ is calculated from

$$\psi_{n\mathbf{k}}^{(1)}(\mathbf{r}) = \sum_{m \neq n} U_{nm\mathbf{k}}^{(1)} \phi_{m\mathbf{k}}^{\text{KS}}(\mathbf{r}), \quad (8)$$

$$U_{nm\mathbf{k}}^{(1)} = \frac{\langle n \mathbf{k} \alpha | \Sigma^{\text{COHSEX}}(s_1, s_2) - V^{\text{xc}} \delta_{s_1, s_2} | m, \mathbf{k}, s_2 d \rangle}{\epsilon_{n\mathbf{k}} - \epsilon_{m\mathbf{k}}}. \quad (9)$$

Fig. 3 displays the values of the coefficients $|U_{nm\mathbf{k}}^{(1)}|$. Only the Γ_6 and Γ_7 states show a contribution to the others' COHSEX wavefunctions to first order. However, the largest contribution is less than 0.1 percent of the zero-order contribution, so the Kohn-Sham states are indeed good approximations to the quasiparticle states.

To better understand the ordering of the electronic states at the Γ point, the bandstructure in DFT is calculated with non-relativistic and scalar-relativistic pseudopotentials. Scalar-relativistic pseudopotentials neglect spin-orbit coupling but include the physics of the Darwin term and the relativistic mass correction, which are both significant for Hg s states. The non-relativistic pseudopotentials neglect these terms. Fig. 4 shows that the non-relativistic pseudopotentials give a bandstructure typical for a zincblende material with

light atoms, where an s -like Γ_1 state is placed E_g above occupied Γ_{15} states. Incorporating the Darwin and relativistic mass-correction terms, however, the Γ_1 lowers below the Fermi energy (Fig. 5). The p - d hybridized Γ_{15} states then split to form parabolic conduction and valence bands that are degenerate at Γ , indicating a zero-gap semimetallic state. Incorporating spin-orbit coupling breaks this degeneracy, and the states can be identified as belonging to either the Γ_7 or Γ_8 representations. The schematic of the changing ordering of the energies upon inclusion of scalar relativistic effects and spin-orbit coupling is shown in Fig. 6a.

Adding the quasiparticle energy correction to the band gap, Δ^{GW} (Fig. 6b), places the Γ_1 state high above the Fermi energy such that scalar relativistic effects do not lower the state below the Fermi energy. Turning on spin-orbit coupling then splits the occupied Γ_{15} states into the Γ_7 and Γ_8 states, with the Γ_7 state higher in energy. ,

IV. CONCLUSION

The bandstructure of β -HgS near the Fermi energy calculated by the the FR- GW approach indicates that the order of the states differs from that predicted by fully-relativistic DFT calculations. While DFT gives an ordering of the bands Γ_6 , Γ_8 , Γ_7 , the present FR- GW quasiparticle energies at the Γ -point is ordered Γ_8 , Γ_7 , Γ_6 . This ordering of the states indicates a topologically trivial narrow band gap semiconductor.

The value of the band gap calculated within FR- GW is 0.10 eV, which compares favorably to the value of 0.11 eV from experiment[34], and the calculated value of the electron effective mass is $0.07 m_e$, which agrees well with the range of values cited in experiment of 0.04 - $0.07 m_e$ [4, 34]. The ordering is reproduced with other approaches of treating the frequency-dependence in the one-shot GW approach, the COHSEX and GPP methods. The possible deviation of the Kohn-Sham orbital basis from the true quasiparticle states, estimated by the COHSEX approximation to the self-energy, indicates that the use of the Kohn-Sham states is accurate to within 0.1 percent.

The reversal of the band inversion predicted in DFT can be understood in terms of the band gap problem. The underestimation of the band gap places the s -like Γ_6 state too low in energy, such that it becomes occupied due to the strength of its change in energy upon incorporation of the relativistic mass correction and Darwin terms captured in scalar- and

fully-relativistic pseudopotentials. The correction to the band gap from *GW* calculations raise its energy sufficiently to place it above the Fermi level.

V. ACKNOWLEDGMENTS

The authors would like to thank Felipe H. da Jornada, Mauro Del Ben, and Jack Deslippe for useful discussions. This work was supported by National Science Foundation Grant No. DMR10-1006184 and by the Director, Office of Science, Office of Basic Energy Sciences, Materials Sciences and Engineering Division, U.S. Department of Energy under Contract No. DE-AC02-05CH11231. within the Nanomachines Program (KC1203) and within the Theory of Materials Program (KC2301). Computational resources have been provided by the DOE at Lawrence Berkeley National Laboratory's NERSC facility.

-
- [1] M. Rohlfing and S. G. Louie, Quasiparticle band structure of hgse, *Physical Review B* **57**, R9392 (1998).
 - [2] A. Svane, N. E. Christensen, M. Cardona, A. N. Chantis, M. van Schilfgaarde, and T. Kotani, Quasiparticle band structures of β -hgs, hgse, and hgte, *Phys. Rev. B* **84**, 205205 (2011).
 - [3] R. Sakuma, C. Friedrich, T. Miyake, S. Blügel, and F. Aryasetiawan, *gw* calculations including spin-orbit coupling: Application to hg chalcogenides, *Phys. Rev. B* **84**, 085144 (2011).
 - [4] R. Zallen and M. Slade, Plasma edge and band structure of cubic hgs, *Solid State Communications* **8**, 1291 (1970).
 - [5] P. Hohenberg and W. Kohn, Inhomogeneous electron gas, *Phys. Rev.* **136**, B864 (1964).
 - [6] W. Kohn and L. J. Sham, Self-consistent equations including exchange and correlation effects, *Phys. Rev.* **140**, A1133 (1965).
 - [7] A. Delin, First-principles calculations of the ii-vi semiconductor β -hgs: Metal or semiconductor, *Phys. Rev. B* **65**, 153205 (2002).
 - [8] F. m. c. Viot, R. Hayn, M. Richter, and J. van den Brink, Metacinnabar (β -hgs): A strong 3d topological insulator with highly anisotropic surface states, *Phys. Rev. Lett.* **106**, 236806 (2011).

- [9] F. m. c. Viot, R. Hayn, M. Richter, and J. van den Brink, Engineering topological surface states: Hgs, hgse, and hgte, [Phys. Rev. Lett. **111**, 146803 \(2013\)](#).
- [10] J. Vidal, X. Zhang, L. Yu, J.-W. Luo, and A. Zunger, False-positive and false-negative assignments of topological insulators in density functional theory and hybrids, *Physical Review B* **84**, 041109 (2011).
- [11] A. Fleszar, *Dielectric response in semiconductors: theory and applications*, Ph.D. thesis, University of Trieste (1985).
- [12] B. A. Bernevig, T. L. Hughes, and S.-C. Zhang, Quantum spin hall effect and topological phase transition in hgte quantum wells, *Science* **314**, 1757 (2006).
- [13] P. Scherpelz, M. Govoni, I. Hamada, and G. Galli, Implementation and validation of fully relativistic gw calculations: Spin-orbit coupling in molecules, nanocrystals, and solids, *Journal of Chemical Theory and Computation* **12**, 3523 (2016).
- [14] J. P. Perdew and A. Zunger, Self-interaction correction to density-functional approximations for many-electron systems, [Phys. Rev. B **23**, 5048 \(1981\)](#).
- [15] F. Aryasetiawan and S. Biermann, Generalized hedin's equations for quantum many-body systems with spin-dependent interactions, [Phys. Rev. Lett. **100**, 116402 \(2008\)](#).
- [16] M. S. Hybertsen and S. G. Louie, Electron correlation in semiconductors and insulators: Band gaps and quasiparticle energies, [Phys. Rev. B **34**, 5390 \(1986\)](#).
- [17] P. Giannozzi, S. Baroni, N. Bonini, M. Calandra, R. Car, C. Cavazzoni, D. Ceresoli, G. L. Chiarotti, M. Cococcioni, I. Dabo, A. D. Corso, S. de Gironcoli, S. Fabris, G. Fratesi, R. Gebauer, U. Gerstmann, C. Gougoussis, A. Kokalj, M. Lazzeri, L. Martin-Samos, N. Marzari, F. Mauri, R. Mazzarello, S. Paolini, A. Pasquarello, L. Paulatto, C. Sbraccia, S. Scandolo, G. Sclauzero, A. P. Seitsonen, A. Smogunov, P. Umari, and R. M. Wentzcovitch, Quantum espresso: a modular and open-source software project for quantum simulations of materials, [Journal of Physics: Condensed Matter **21**, 395502 \(2009\)](#).
- [18] D. R. Hamann, Optimized norm-conserving vanderbilt pseudopotentials, [Phys. Rev. B **88**, 085117 \(2013\)](#).
- [19] M. van Setten, M. Giantomassi, E. Bousquet, M. Verstraete, D. Hamann, X. Gonze, and G.-M. Rignanese, The pseudodojo: Training and grading a 85 element optimized norm-conserving pseudopotential table, [Computer Physics Communications **226**, 39 \(2018\)](#).

- [20] K. Lejaeghere, G. Bihlmayer, T. Björkman, P. Blaha, S. Blügel, V. Blum, D. Caliste, I. E. Castelli, and S. J. Clark, Reproducibility in density functional theory calculations of solids, *Science* **351**, [10.1126/science.aad3000](https://doi.org/10.1126/science.aad3000) (2016).
- [21] M. L. Tiago, S. Ismail-Beigi, and S. G. Louie, Effect of semicore orbitals on the electronic band gaps of si, ge, and gaas within the gw approximation, *Physical Review B* **69**, 125212 (2004).
- [22] O. Madelung, *Semiconductors: Data Handbook* (Springer Berlin Heidelberg, 2004).
- [23] J. Deslippe, G. Samsonidze, D. A. Strubbe, M. Jain, M. L. Cohen, and S. G. Louie, Berkeleygw: A massively parallel computer package for the calculation of the quasiparticle and optical properties of materials and nanostructures, *Computer Physics Communications* **183**, 1269 (2012).
- [24] C.-D. Spataru, *Electronic Excitations in Solids and Novel Materials*, Ph.D. thesis, University of California at Berkeley (2004).
- [25] R. W. Godby, M. Schlüter, and L. J. Sham, Self-energy operators and exchange-correlation potentials in semiconductors, *Phys. Rev. B* **37**, 10159 (1988).
- [26] R. Car, E. Tosatti, S. Baroni, and S. Leelaprute, Dielectric band structure of crystals: General properties and calculations for silicon, *Phys. Rev. B* **24**, 985 (1981).
- [27] M. Govoni and G. Galli, Large Scale GW Calculations, *J. Chem. Theory Comput.* **11**, 2680 (2015), pMID: 26575564.
- [28] M. Del Ben, F. H. da Jornada, G. Antonius, T. Rangel, S. G. Louie, J. Deslippe, and A. Canning, Static subspace approximation for the evaluation of G_0W_0 quasiparticle energies within a sum-over-bands approach, *Phys. Rev. B* **99**, 125128 (2019).
- [29] B. D. Malone and M. L. Cohen, Quasiparticle semiconductor band structures including spin-orbit interactions, *Journal of Physics: Condensed Matter* **25**, 105503 (2013).
- [30] J. Deslippe, G. Samsonidze, M. Jain, M. L. Cohen, and S. G. Louie, Coulomb-hole summations and energies for g w calculations with limited number of empty orbitals: A modified static remainder approach, *Physical Review B* **87**, 165124 (2013).
- [31] S.-H. Wei and A. Zunger, Role of metal d states in ii-vi semiconductors, *Physical Review B* **37**, 8958 (1988).
- [32] C. E. Moore, *Atomic Energy Levels*, Vol. 3 (Circular of the National Bureau of Standards, Washington, DC, 1958).

- [33] C. E. Moore, *Atomic Energy Levels*, Vol. 1 (Circular of the National Bureau of Standards, Washington, DC, 1958).
- [34] K. Dybko, W. Szuszkiewicz, E. Dynowska, W. Paszkowicz, and B. Witkowska, Band structure of β -hgs from shubnikov–de haas effect, *Physica B: Condensed Matter* **256**, 629 (1998).
- [35] This was first noted in Ref. 2.
- [36] S. B. Zhang, D. Tománek, M. L. Cohen, S. G. Louie, and M. S. Hybertsen, Evaluation of quasiparticle energies for semiconductors without inversion symmetry, *Phys. Rev. B* **40**, 3162 (1989).

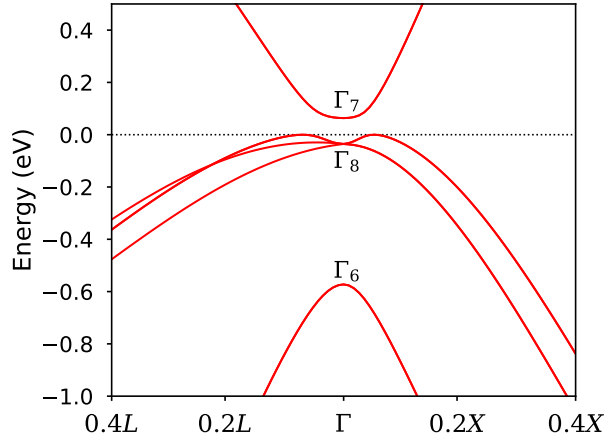


FIG. 1: The fully-relativistic DFT bandstructure of β -HgS. The states at the Γ -point, in increasing energy, are Γ_6 , Γ_8 , Γ_7 .

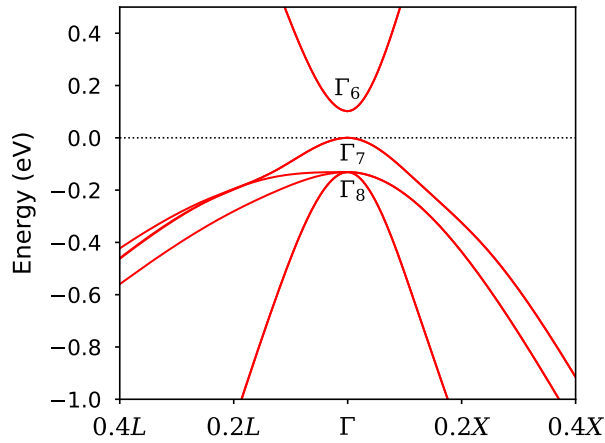


FIG. 2: The quasiparticle bandstructure of β -HgS, computed at the FR-GW level using the contour deformation method. The states at the Γ -point, in increasing energy, are Γ_8 , Γ_7 , Γ_6 .

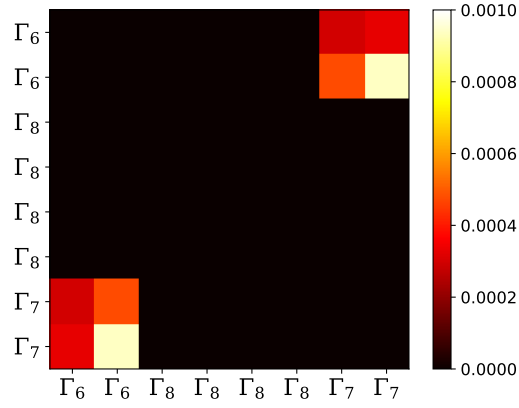


FIG. 3: The first-order correction to each COHSEX wavefunction (rows), within the Kohn-Sham orbital basis (columns). The maximum off-diagonal contribution is less than 0.1 percent.

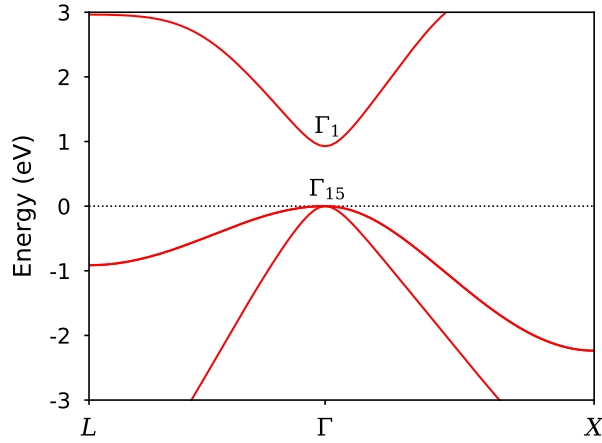


FIG. 4: The non-relativistic DFT bandstructure of β -HgS. The states at the Γ point are ordered Γ_{15} , Γ_1 , as in a conventional zincblende structure.

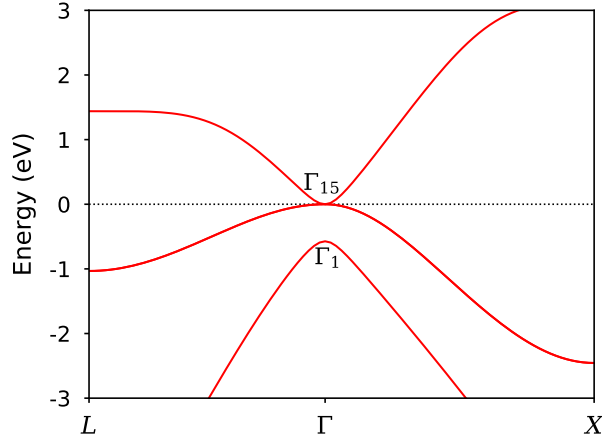


FIG. 5: The scalar-relativistic DFT bandstructure of β -HgS. The degenerate states at $E_F = 0$ belong to the Γ_{15} representation, and the lower occupied state belongs to Γ_1 .

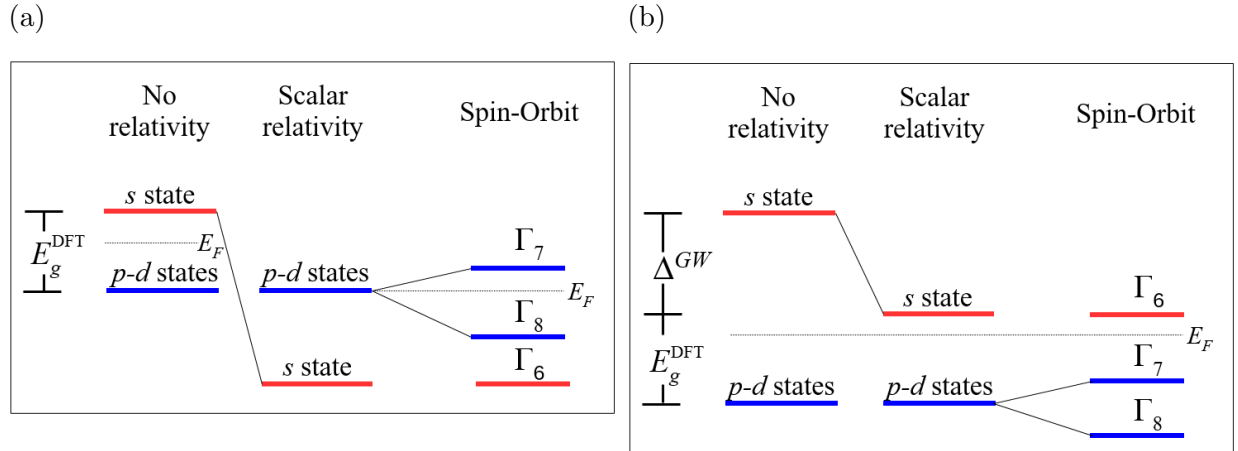


FIG. 6: (a) A schematic of the single-particle energies computed within DFT, first neglecting relativistic effects (left), then including scalar relativistic effects (middle), and spin-orbit coupling (right). The p - d hybridized states are at the Fermi energy when including scalar relativistic effects. (b) A schematic of the single-particle energies when including corrections from GW quasiparticle calculations. The s state lowers in energy when including scalar relativistic effects but now remains above the Fermi energy.

TABLE I: A comparison of the results for interband gaps near the Fermi energy from the literature.

	E_0 (eV)	Δ^{SOC} (eV)	E_g (eV)	Basis set
Present Work (FR-GW)	0.23	-0.13	0.10	Plane-wave (PW)
$GW+\text{SOC}^{\text{a}}$	0.18	-0.12	0.06	Gaussian+PW
hybrid-QSGW ^b	0.37	-0.07	0.31	LMTO
FR-GW ^c	-0.02	-0.19	0.02	FLAPW
FR-GW ^d	-0.02	-0.10	0.02	PW

^a Ref. 11

^b Ref. 2

^c Ref. 3

^d Ref. 13

TABLE II: Interband gaps near the Fermi energy for β -HgS. From DFT, the four-fold Γ_8 states are higher in energy than the two-fold s -like Γ_6 states. With the inclusion of self-energy effects (COHSEX, GPP, or Contour deformation), the Γ_8 states are lower in energy than the now-unoccupied Γ_6 states.

	E_0 (eV)	Δ^{SOC} (eV)	E_g (eV)
DFT	-0.54	-0.10	0.10
COHSEX	0.92	-0.12	0.80
GPP	0.37	-0.15	0.22
Contour deformation	0.23	-0.13	0.10